Received: 12 October 2020 | Revised: 19 March 2021 | Accepted: 21 March 2021

DOI: 10.1002/app.50783

ARTICLE

Applied Polymer SCIENCE WILEY

Time-dependent properties of graphene nanoplatelets reinforced high-density polyethylene

Zainab Al-Maqdasi[1] | Liva Pupure[1,2] | Guan Gong[3] | Nazanin Emami[1] | Roberts Joffe[1]

[1]Department of Engineering Sciences and Mathematics, Luleå University of Technology, Luleå, Sweden

[2]Riga Technical University, Institute of Construction and Reconstruction, Riga, Latvia

[3]RISE SICOMP AB, Composite materials and product development, Piteå, Sweden

Correspondence
Zainab Al-Maqdasi, Luleå University of Technology, SE 97187 Luleå, Sweden.
Email: zainab.al-maqdasi@ltu.se

Funding information
Horizon 2020, Grant/Award Number: 777810; Interreg Nord; Luleå Tekniska Universitet, Grant/Award Number: Smart Machines and Materials

Abstract

The deformation of polymers at constant applied stress is one of their major drawbacks, limiting their use in advanced applications. The study of this property using classical techniques requires extensive testing over long periods of time. It is well known that reinforced polymers show improved behavior over time compared to their neat counterparts. In this study, the effect of adding different amounts of graphene nanoplatelets (GNPs) on the time-dependent properties of high-density polyethylene (HDPE) is investigated using short-term creep tests and load/unload recovery tests. The results are discussed in terms of the test profile and the influence of loading history. Viscoplasticity/viscoelasticity analysis is performed using Zapas model and by comparing creep, creep compliance and pure viscoelasticity curves. The results show that the reinforcement of 15 wt% GNP have the most significant effect on the time-dependent behavior, reducing the strain by more than 50%. The creep compliance curves show that nano-reinforced HDPE behaves nonlinearly viscoelastically even at very low stresses. In addition to demonstrating the effect of nano-reinforcement, the discussion of the results concludes that the influence of loading history can be quite significant and should not be neglected in the design and evaluation of material behavior.

KEYWORDS

graphene and fullerenes, mechanical properties, theory and modeling, thermoplastics, viscosity and viscoelasticity

1 | INTRODUCTION

Interest in the use of polymers and their composites as lightweight, chemical- and corrosion-resistant alternatives to metals remains strong and continues to grow, for example, in the automotive industry,[1] tribological applications,[2] and construction.[3] With the progress in nanotechnology, new multiscale, multifunctional polymeric materials with nanoscale reinforcements are being developed, and research continues to characterize their physical, thermal, and mechanical properties. Of these materials, polymers doped with nanoscale carbon derivatives (e.g., carbon nanotubes and graphene or graphene derivatives) are emerging as candidates for the automotive industry and other advanced applications, such as flexible electronics and smart structures.[4]

A general characteristic of polymers is their viscoelastic behavior and the dependence of their properties on time. A polymeric material subjected to a constant load over a long period of time exhibits large deformations (creep), leading to failure at stresses below the tensile strength. In applications, this determines the life of a component and the need to replace it. Reinforcing polymers is one way to enhance the creep resistance and extend service life that eliminate the need for frequent replacement, resulting in reduced plastic waste. Even polymers with the nano-reinforcement exhibit nonlinear behavior,[5] but the degree of nonlinearity in the viscoelastic response (in Polyamide 66 [PA66]) was found to be reduced with the size of nanoparticles that in return contribute to a better improvement in the creep resistance.[6] The mechanism of altering the time-dependent response upon incorporating nano-reinforcement is best explained by the restricted mobility of polymer chains by the effect of rigid inclusions.[7] One of the phenomena which are crucial for the performance of materials over time is the development of irreversible deformation caused by microdamage or/and viscoplasticity. However, research on the time-dependent properties of nanocomposites is still quite limited,[5,8–10] compared to the extensive research on other mechanical properties. This is due to the complexity and lengthy times of traditional experimental procedures for evaluating such properties. Moreover, fundamental simulation studies at the molecular level require accurate and detailed knowledge of nanoparticles and the polymer properties, which are usually difficult to obtain. Such studies deal with idealized systems that are far from reality when they are produced commercially.

Among the different carbon derivatives, graphene sheets were reported to have the most significant positive effect on the creep resistance of the host polymer.[11,12] Single-layer graphene is a 2D material with a thickness of one carbon atom that has remarkable mechanical, thermal and electrical properties.[13–15] Doping polymers with this material can lead to a significant improvement in mechanical properties together with additional functionality derived from the intrinsic properties of graphene. However, the production routes for single-layer graphene are high energy-consuming and uneconomical for large scale systems. Graphene Nanoplatelets (GNPs), which consist of multiple layers of graphene sheets, are alternative 2D materials that can be fabricated using lower-cost methods suitable for upscaling.[16,17] Due to the large aspect ratio of these 2D nanomaterials they can be used to modify polymers resulting in a notable improvement in the mechanical properties,[18] compared to neat counterparts even at relatively small loadings,[19] provided that a suitable processing technique is used that directly affects the quality of the particle dispersion.[20,21]

Modeling and predicting the behavior of materials over time helps avoid extensive and time-consuming testing. Conventional models used for predicting the time-dependent behavior of viscoelastic materials are the empirical models such as Norton's power law,[22] and its modifications or constitutive models in which damage accumulation is taken into account, and extensive experiments for parametric identification are avoided.[23] A viscoplastic (VP) model proposed by Zapas et al.[24] has been successfully used to describe the VP strain evolution in different materials.[25–29] In this model, the VP strain is written in terms of a stress-dependent integral, with parameters determined in creep and strain recovery tests. However, it has not been studied to describe the behavior of nano-reinforced polymers.

Despite the large number of studies investigating the effect of nanoplatelets on the mechanical properties of thermoplastic polymer nanocomposites, less focus has been placed on the combination of high-density polyethylene (HDPE)/GNP produced by melt blending.[19] Besides, the use of a commercial masterbatch as a feedstock for easily scalable production is being explored. This study investigates the time-dependent behavior of HDPE doped with GNPs using a masterbatch in a melt blending process without using a compatibilizer. The focus of the work is to (1) evaluate the time-dependent response of HDPE at different GNPs loading and with different loading scenarios; (2) evaluate the applicability of a previously developed model to predict the creep of nanocomposites and validate the modeling approach in general; and (3) characterize the viscoelastic response of these materials in terms of linearity/nonlinearity. The work presented here is a comprehensive investigation of the time-dependent response with respect to viscoplastic and viscoelastic components performed at relatively short time intervals. This is done by experimentally characterizing the irreversible, that is, viscoplastic (VP) strain evolution and identifying the VP model based on these measurements. The results and conclusions are supported by complementary tests for validation. A quantitative analysis of the effect of GNPs on the viscoelasticity of HDPE was also performed. The approach of separating the VP and VE responses allows for future prediction of complex loading profiles, facilitated by the extracted modeling parameters.

2 | EXPERIMENTAL

Commercial HDPE (MG9647S, BOREALIS) pellets were used as reference material and matrix in the prepared nanocomposites. The reinforcement is presented in the form of commercial masterbatch pellets. The HDPE-based masterbatch containing 35 wt% GNPs

(heXo HDPE1-V20/35, NanoXplore) was used to obtain HDPE with various GNP contents by 'diluting' with the pure polymer to obtain the required GNP content. The GNPs in the masterbatch are in the form of 40 layers graphene sheets making up a thickness of 20 nm, lateral flake size of 50 μm and an average surface area of 30 m^2/g. Based on the manufacturer's technical datasheets,[30] these platelets are functionalized only at the edges with carbonyl and hydroxyl groups that make up less than 2% by atomic weight to enhance their compatibility with the polymer. This functionalization has eliminated the need to use additional coupling agent or compatibilizer during the processing.[31] Since these are commercial products, particles were not further modified or characterized as it is not the scope of the current study, and these characterizations have already been performed by the manufacturer and can be found in the technical datasheets.[30] The choice of this type of reinforcement is based on their suitability for developing polymer with added functionality for multifunctional composites (with thermal or electrical functionality besides the structural characteristics) in a previous work by the authors.[31] The number of functional groups is kept at a minimum and are present only at the edges in order to preserve the conductive characteristic of graphene sheets. It is also the reason behind the selection of high content of GNPs in the investigated materials (see the following paragraph) since the percolation threshold for conductivity is relatively high for highly crystalline thermoplastics processed by melt blending.[32]

The nanocomposites were manufactured by melt compounding in a co-rotating twin-screw extruder (ZSK25, Krupp Wener & Pfleiderer GmbH) followed by compression molding using a conventional 310-ton press (Fjellman). It is worth noting that the term 'nanocomposite' usually refers to composites modified with nano-sized particles even if they end up being present in the microscale due to their re-agglomeration during processing. This convention is further used in the rest of the manuscript. Specimens were cut from the pressed plates using waterjet and thoroughly dried for 8 hr at 80 °C. Further details of the composite processing are not elucidated here as this information is presented in a previous publication.[31] The content of GNP in the resulting composites were 2, 6, and 15 wt%. Neat HDPE matrix was used as reference material, but it was pressed directly from the granules without extrusion. It is the intention of this study to present comparative trends in terms of reinforcement content rather than quantitative values; therefore, differences arising from the different processing techniques of the neat polymer and the nanocomposites are neglected when evaluating the overall trends. It is logical that processing the neat polymer in the extruder could lead to a decrease in its properties (caused by possible chain shortening due to cleavage) and would lower the initial values of the reference; therefore, any improvement resulting from the addition of the reinforcement would only become more extensive when compared to larger initial differences based on Equation (1).

$$\%\ improvement\ \mathrm{n}\ in\ X = \frac{(X_2 - X_1)}{X_1} \times 100\%, \qquad (1)$$

in which X_2 is the property of the modified nanocomposite, and X_1 is the property of the reference polymer.

Creep tests (in tension) were performed on electromechanical tensile machine Instron 3366 equipped with 10 kN load cell and pneumatic grips following the test sequence presented in Figure 1. Standard Instron extensometer 2620–601 with 50 mm base was used to measure axial strains ε_x, whereas lateral strains, ε_y, resulting from the lateral contraction of the sample by the Poisson's effect, were measured by general-purpose strain gauges (EA-06-015EH-120/LE, from Micro-Measurements). Rectangular specimens (70 mm in gauge length, 18 mm in width) were subjected to a sequence of tensile loading ramps each consisting of uploading to constant stress (loading was done in displacement-controlled mode with a rate of 3.5 mm/min which corresponds to a strain rate of 5%/min); keeping the stress constant for a fixed time (creep); unloading (the same rate as loading) the specimen and waiting for viscoelastic strain recovery (to measure residual strains). The duration of creep loading in a ramp was 10, 20, 30 and 60 min, with a total creep test time of 2 hr. The applied stress levels in the creep test were 7.5, 10, 12.5 and 15 MPa which correspond to 30% to 60% of the maximum tensile stress of HDPE (22 MPa). Tests were performed on a single specimen of each material in an increasing order of the applied stress to minimize the scatter and the influence of damage on results as was previously established.[28] Each loading period in the ramp was followed by the recovery period of eight times (×8) longer than the loading time. During strain recovery, the load was kept constant at 4 N. The specimen was not unloaded entirely (to zero load) due to technical reasons. However, the 4 N value was very small and corresponds to less than 1% of the maximum load applied at smallest stress level (7.5 MPa) of neat polymer (the value is lower than 1% at higher stress levels). At the end of the recovery, residual strains in two directions, ε_x^{VP} (further in the paper referred to as axial) and ε_y^{VP} (denoted as lateral), were considered as viscoplastic.

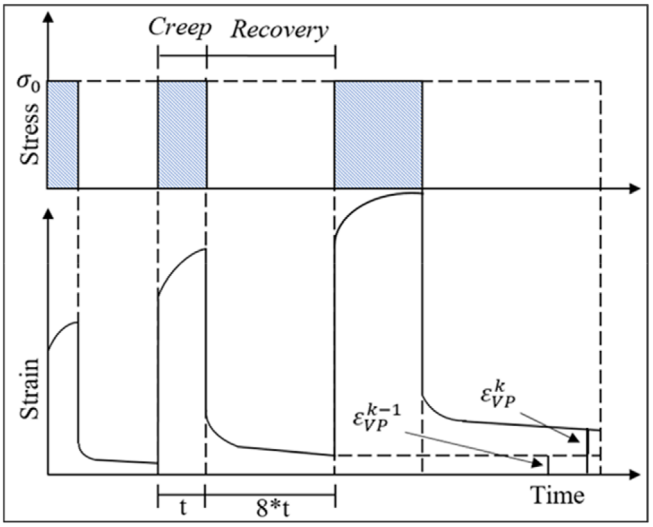

FIGURE 1 Schematics of the test sequence and residual (viscoplastic) strains at the end of the recovery [Color figure can be viewed at wileyonlinelibrary.com]

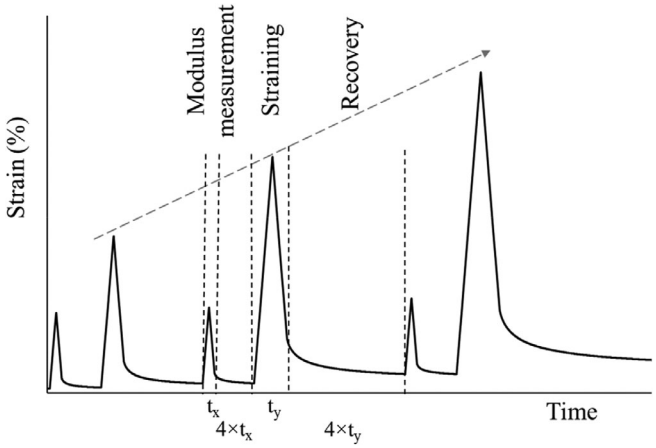

FIGURE 2 Schematic of the loading-unloading-recovery test; the small peaks correspond to the 0.2% strain step for the modulus calculation, and the larger peaks are the loading ramps, which were varied in steps from 0.4 to 6%

After the material has been subjected to high stresses, the materials' elastic properties (stiffness) may be affected, and filler-filler interaction may occur, especially with high amounts of GNPs. To evaluate the significance of damage developed at high stresses, the dependence of the elastic modulus on the previously applied maximum strain/stress was measured in a loading-unloading-recovery test. A cycle consists of loading to a strain of 0.2%, subsequent unloading to a load level of 5 N, and reloading to a predetermined strain level. In the following step of a cycle, the strain was varied: 0.4, 0.6, 0.8, 1, 1.5, 2, 3, 4, 5, and 6% relative to the residual strains from the previous step. After each unloading step, the specimen was allowed to recover the reversible strains for a period of time ×4 longer than the time required to load and unload the specimen. The cyclic tests were performed in displacement-controlled mode at 2 mm/min (equivalent to 2%/min) on the same setup used for the creep tests. Modulus was calculated from the unloading segment of the 0.2% strain step between the strain range of 0.1–0.05%.

The evolution of accumulated strains makes it challenging to set constant test criteria in terms of strain. For example, after an accumulated strain of 1%, the next loading step would also be shifted by 1%. Also, it would not be possible to maintain the same strain interval for stiffness calculation in all cycles. To solve the first problem, the loading ramp was set relative to the residual strain of the previous cycle. As for the stiffness calculation, the stress levels corresponding to the strains in the first loading-unloading ramp were noted and then used in all subsequent steps, that is, the stiffness was calculated from the slope of the unloading segment in the range between ∼0.25 MPa (corresponding to 0.05% strain in the first step) and ∼ 1.12 MPa (corresponding to 0.1% strain in the first step). Figure 2 shows the schematic of the testing procedure with the loading and recovery segments.

To demonstrate the morphology of the prepared materials, scanning electron microscopy (SEM, JEOL JCM-6000 Neoscope) was performed with an electron acceleration of 15 kV. The samples were broken in liquid nitrogen, and the broken surface was sputter-coated with gold before microscopic examination.

3 | MODELING OF NONLINEAR DEFORMATION BEHAVIOR

The strain response of materials under load can be separated into the irreversible viscoplastic (ε_{VP}) and the reversible viscoelastic (ε_{VE}) strains developed under load. Both can be influenced by possible microdamage introduced into the microstructure leading the total strain (ε) to be written as follows:

$$\varepsilon(\sigma,t) = d(\sigma_{max})\varepsilon_{VE}(\sigma,t) + d(\sigma_{max})\varepsilon_{VP}(\sigma,t), \qquad (2)$$

where the strain (ε) is a function of stress (σ) and time (t). In Equation (2), parameter d represents the effect of damage introduced at the maximum applied stress (σ_{max}).

The viscoplasticity was characterized using model by Zapas and Crissman,[24] where VP strain growth during loading with specified time dependence of the applied stress is given by:

$$\varepsilon_{VP}(\sigma,t) = C_{VP}\left\{\int_0^{\frac{t}{t^*}}\left(\frac{\sigma(\tau)}{\sigma*}\right)^M d\tau\right\}^m, \quad (3)$$

where C_{VP}, M and m are constants to be determined experimentally, σ^* is arbitrary chosen stress value, $\frac{t}{t^*}$ is normalized time and t^* is an arbitrarily chosen characteristic time constant. For simplicity and to obtain dimensionless parameters, values of σ^*=1 MPa and t^*=120 min (equal to total creep time) were used in this study.

Limited material was available for experiments, and thus, the methodology described in work by Pupure et al.[28] was employed in order to obtain the maximum amount of information for experimental material constants from the least number of tested specimens. This method allows full characterization of viscoplasticity using only one specimen. However, this methodology is material-sensitive, and thus some preliminary investigations have been performed to set test criteria and are discussed in the following section. Due to the previous loading history, the parameter identification becomes more complicated. At k-th stress level $n_k\sigma_0$ (for the first stress level the $n_1 = 1$) and with the same total duration time of creep Δt_0 for previous stress levels, VP strain can be obtained as follows:

$$\varepsilon_{VP}(n_k,t) = C_{VP}\sigma_0^{mM}\left(\frac{\Delta t_0}{t^*} + n_2^M\frac{\Delta t_0}{t^*} + n_3^M\frac{\Delta t_0}{t^*} + \ldots + n_k^M\frac{t-(k-1)\Delta t_0}{t^*}\right)^m, \quad (4)$$

Since t^* is an arbitrary chosen constant, the choice of $t^* = \Delta t_0$ reduces Equation (4) to:

$$\varepsilon_{VP}(n_k,t) = C_{VP}\sigma_0^{mM}\left(1 + n_2^M + n_3^M + \ldots + n_k^M\frac{t-(k-1)\Delta t_0}{t^*}\right)^m, \quad (5)$$

Applying natural logarithm of both sides of Equation (5) renders the following relationship:

$$ln(\varepsilon_{VP}(n_k,t)) = ln\left(C_{VP}\sigma_0^{mM}\right) + m\,ln\left(1 + n_2^M + n_3^M + \ldots + n_k^M\frac{t-(k-1)\Delta t_0}{t^*}\right), \quad (6)$$

From this equation follows that experimental relationship between VP strain and time $ln(\varepsilon_{VP})$~$ln(f(n_i, M, t))$ has to be linear for all stress levels. Thus, the first step is to find M value when for all the stress levels the data points are "linearized". These data can be fitted with function $y = mx + c$, thus obtaining a first approximation of parameter m and C_{VP}. By further adjusting the parameters, to obtain the best overall fit (m, C_{VP} values have to be the same for all stress levels), the correct values for viscoplasticity law can be obtained. It has been seen that fitting of data at higher stress levels is significant for more accurate VP parameter identification. By doing so, any discrepancy of the fitted curves from the experimental results becomes less significant at lower stress levels or strain values. It should also be noted that the fine-tuning of the fitting parameters is done by visual evaluation of the curves fitting to the experimental data.

Afterwards, the VP strain can be subtracted from the total amount of strain to obtain pure VE strain. The VP strain was removed with the method described by Nordin and Varna.[25] This methodology allows the use of actual VP strain of experiment in the subtraction process, thus reducing the effect of scattering between different experiments. The amount of VP strain removed from the individual test would be the same as experimentally measured.

During the first creep loading step, viscoplasticity is removed with the following expression:

$$\varepsilon_{VP}^1(t) = \varepsilon_{VP}^c\left(\frac{t}{\Delta t_1}\right)^m, \quad (7)$$

where ε_{VP}^c is the VP strain accumulated during loading of the first step with a total duration of Δt_1. Afterwards, due to previous loading history, removal of viscoplasticity is done according to this expression:

$$\varepsilon_{VP}^k(t) = \left\{\left(\varepsilon_{VP}^{k-1}\right)^{\frac{1}{m}} + \left[\left(\varepsilon_{VP}^k\right)^{\frac{1}{m}} - \left(\varepsilon_{VP}^{k-1}\right)^{\frac{1}{m}}\right]\frac{t-t_{k-1}}{t_k-t_{k-1}}\right\}^m, \quad (8)$$

where t_{k-1} is the time at the beginning of the current loading step and t_k is the time at the end of the current loading step.

4 | RESULTS AND DISCUSSIONS

4.1 | Results of preliminary investigations

It is well known that polymers fail by creep at stresses lower than their ultimate tensile strength. Therefore, to avoid failure of the specimens during the creep test, the selection of creep stresses is based on the breaking stress. The materials prepared have the tensile properties shown in Table 1,[31] upon which the creep stresses were selected between 30% and 60% of the maximum tensile stress of

TABLE 1 Tensile properties of HDPE and its nanocomposites

Property/material	HDPE+0%GNP	HDPE+2%GNP	HDPE+6%GNP	HDPE+15%GNP
Modulus [GPa]	1.89 ± 0.06	2.11 ± 0.11	2.49 ± 0.05	3.85 ± 0.19
Maximum Stress [MPa]	22.47 ± 0.57	22.71 ± 0.35	23.46 ± 0.32	26.40 ± 0.53

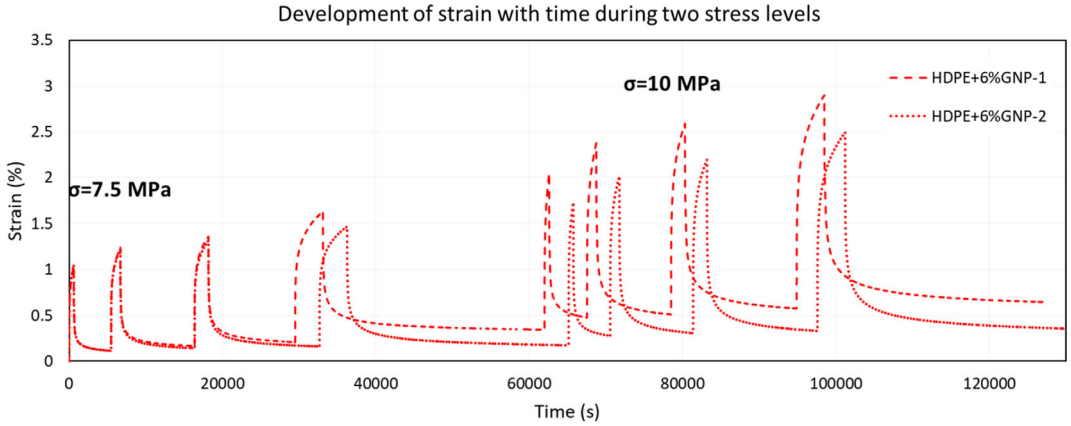

FIGURE 3 Development of strain for two specimens of HDPE+6%GNP at different recovery times at two stress levels (7.5 and 10 MPa) [Color figure can be viewed at wileyonlinelibrary.com]

HDPE. The results show that the strength and modulus increased continuously with the increase of the reinforcement percentage. This was attributed to both the particles' inherited stiffness and the improved compatibility with the polymer due to the functionalization of the platelets at the edges. In addition, the low scatter of the results (all scatter values are within 5% of the mean) could support the applicability of using one specimen that can be representative of the material. Nevertheless, the use of multiple samples for validation purposes is recommended if they are available.

The consistency of samples and the dependency of results on recovery time were investigated utilizing two specimens of the 6% GNP content subjected to different loading profiles. Figure 3 shows that the two specimens are behaving identically at the first three steps when the testing profile was identical, indicating consistency between the different samples. However, when the time of recovery was shorter in one specimen (ramp 4 in Figure 3), the recovery was not completed, and some of the reversible strains were not fully recovered. These strains were carried on to the next stress level causing a discrepancy in the results. Therefore, a recovery time of eight times the loading time was followed during the rest of the experiments.

A further investigation of the influence of loading history was carried out with the loading-unloading-recovery test. For this purpose, an additional specimen from two materials were used, namely HDPE+0%GNP and HDPE +2%GNP. These specimens were loaded to 6% strain in a continuous ramp, and the response was compared to applying the load in several smaller increments. The response was not investigated for all combinations, but the two combinations investigated were sufficient to infer the importance of the loading history and recovery part that should be considered in further investigations. Figure 4(a) shows the graphs for the 2%GNP combination, while Figure 4(b) shows an enlarged section of the initial part of the curves in Figure 4(a). The curves show a clear viscoelastic response represented by the hysteresis loops and a strong dependence of the material behavior on the loading history. The material loaded stepwise to a specific strain level (6%) shows larger strains (resulting from the accumulation of residual strains in each step) compared to direct loading with one step to the same strain. This is also shown numerically in Table 2 for the two combinations of materials at low- and high-stress levels. In a previous study[33] conducted with a similar material (HDPE), the results show no dependence on the loading history. However, in that study, the specimens were not allowed to recover after load removal, so the viscoelastic strains were not fully recovered to show the effect of viscoplasticity. In the current work, time was given for recovery, and viscoplasticity showed a clear dependence on both loading history and recovery time. It can be concluded that the recovery portion is an essential step in the test, which also reflects a more realistic approximation of cases in real applications. It is also worth noting that the stiffening of the material due to the addition of GNPs manifests itself in the higher stress

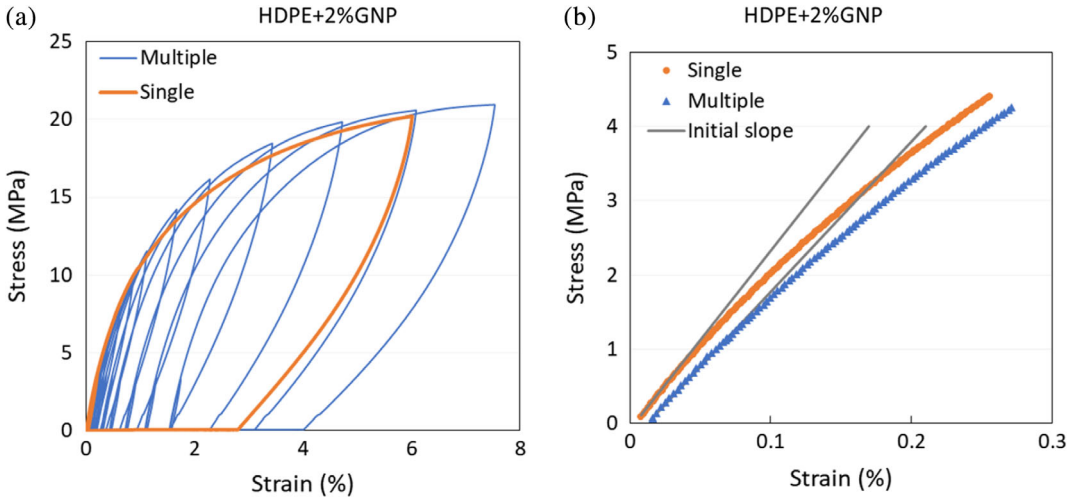

FIGURE 4 Effect of loading history during the loading-unloading-recovery test (a) and enlarged portion of the initial part of the curve (b) [Color figure can be viewed at wileyonlinelibrary.com]

TABLE 2 Effect of the loading history and the GNPs content on the residual strains in loading-unloading-recovery test

Material	HDPE+0%GNPs				HDPE+2%GNPs			
Loading type	Single step		Multiple steps		Single step		Multiple steps	
Stress level [MPa]	3.07	20.23	3.17	20.4	3.66	20.22	3.37	20.92
Residual strain [%]	0.01	1.219	0.011	1.989	0.008	1.15	0.013	2.036

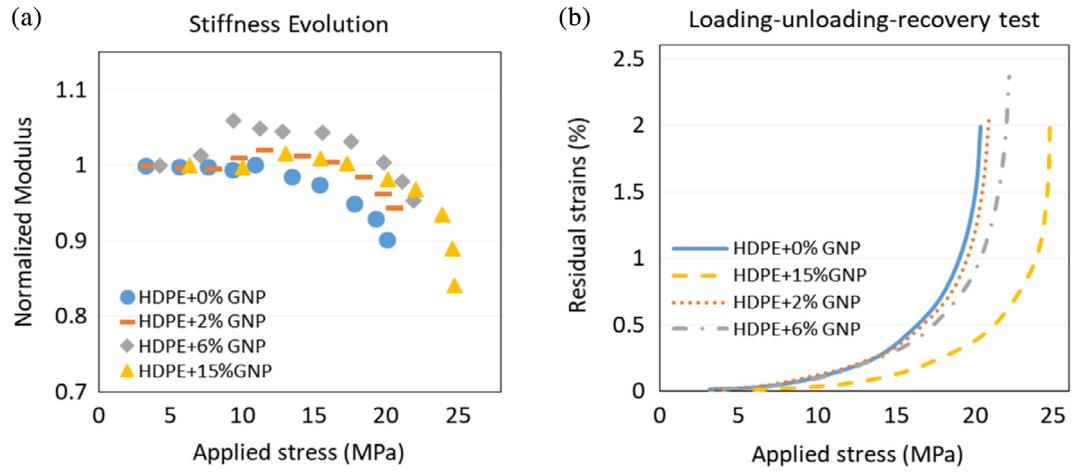

FIGURE 5 (a) stiffness evolution of the different materials with the incremental stress levels; (b) residual strains against maximum applied stress obtained from loading-unloading-recovery test [Color figure can be viewed at wileyonlinelibrary.com]

levels reached at the 6% strains applied, resulting in higher apparent residual strains.

From Figure 4(b), one can also see the nonlinear behavior in these materials even at very low stresses. This performance was also observed for the pure polymer (the curve is shown in Figure S1 in the Supporting Information Document), where the stress at the yield point corresponding to a 0.2% offset strain was only 8 MPa. This is typical behavior for semi-crystalline thermoplastics, which exhibit significant viscoelastic response.[34] This nonlinearity is expected to decrease with the addition of more rigid nanoparticles, but not necessarily disappear completely. Previous studies have shown similar trends for GNP-reinforced polymer nanocomposites, where both elastic and viscoelastic nonlinearity were reduced with the addition of the particles.[6,35] When loaded up to a specific stress/strain, filler-filler interaction and filler layers begin to break and slip. At this point, nonlinearity may increase, especially at higher amounts of filler particles, as more interaction promotes nonlinearity (discussed in the next section).

4.2 | Loading-unloading-recovery test

After each loading step applied to the material, the stiffness was evaluated. The stiffness is normalized to the initial value, and its evolution with the maximum applied stress is shown in Figure 5(a) (a similar figure plotted against strain can be found in Supporting Information, Figure S2). It can be seen that the stiffness of the materials shows no noticeable change up to a stress of 17 MPa. However, after this stress value, the stiffness starts deteriorating and shows a maximum decrease of 20% for the sample with maximum filler content loaded to a stress of 25 MPa. This results from the large plastic deformations suffered by the material when subjected to high stresses (recall that the maximum tensile stress of HDPE+15% GNP is 26.4 MPa). It is worth noting that the stress for the onset of plastic deformation (17 MPa) is higher than the maximum stress level chosen in the creep test (15 MPa). Therefore, it is safe to assume that the damage parameter in (2) is negligible when modeling nonlinearity up to a stress of 17 MPa. At high stresses and large amounts of reinforcement, degradation is assumed to proceed more rapidly due to the expected agglomerations that may act as damage triggers or cause local stress concentrations. This is observed by the steep degradation of the stiffness of the material with 15% GNP at the last three stress levels.

The trend of the change of the irreversible strains by the effect of the addition of GNPs at different stress values obtained from the loading-unloading-recovery test is shown in Figure 5(b). It is clear from the figure that the significant difference in the residual strains is achieved only at the higher GNPs loading (15 wt%). Up until 15 MPa stress level, the other materials showed no notable difference in the accumulation of the residual strains.

4.3 | Morphology

Figure 6 shows the morphology of the studied materials at different GNP loadings as seen under the SEM. Since no rupture occurred during the creep tests at any stress levels or creeping times, the microstructure was investigated on samples cryo-fractured in liquid nitrogen. An interesting difference could be seen when materials are observed at low and high magnifications. At low magnifications, the overall trend shows an increased surface roughening in the presence of the GNPs compared to pure polymer (images c, e, g compared to a, in Figure 6) where the particles introduce torturous routes for the fracture path. On the other hand, the magnified micrographs show more the regions of polymers in focus and in those micrographs the trend is reversed. There is an evident change in the morphology of the polymer from the topological fibrillated surface of the HDPE in Figure 6(a), (b) (indicated by the arraws in (b)), to the smoother surface at higher GNP loadings (6 wt% and 15 wt%) in Figure 6(e)-(g). This behavior of polymer is explained by cryo-state at fracture since the polymer was near its glass transition temperature (−125 °C[36]), thus showing a characteristic more akin to that of brittle polymers. Additionally, the polymer chains between the GNPs become more locally stressed by the effect of the surrounding rigid particles.[37] The effect of the addition of platelets on the fracture behavior of the polymers is still controversial due to the challenges in achieving consistent quality of nanocomposites to study it thoroughly, but positive and negative effects have both been observed.[38] At 2 wt% GNP, the introduced particles could be detected at some sites (e.g., the ones marked at the tip of arrows in Figure 6(d)), but the occurrence of GNP is denser in samples of 6 wt% and 15 wt% GNP contents, see Figure 6(e)-(h). The platelets appear mostly thin and transparent, indicating the presence of well-separated sheets. But thicker, less separated particles could also be spotted, such as the agglomerates at the highest particle content shown in Figure 6(i),(j). However, since no negative effect has been noticed on most of the studied properties, it is assumed that such defects are homogeneously distributed within the volume of material.[31] Generally, rather than a single state, a mixture of different states of the nanoplatelets (aggregates, intercalated, and exfoliated nanoparticles) exist simultaneously in the nanocomposites.[39] However, particles are overall well embedded in the matrix and homogeneously distributed. It is well known that the study of the morphology of nanoparticles themselves under the Transmission Electron Microscope (TEM) rather than Scanning Electron Microscope (SEM) renders more specific details about the exfoliation state of the particles and the possible distance between the graphene sheets within the platelets. However, SEM can give wider observation view and delocalized characteristics of the material in general where the distribution of fillers can better be observed[40] which is more crucial for the current study. The micrographs support findings concerning the improvement of stiffness and the suppression of microdamage due to the absence of gaps and the good compatibility of the platelets with the polymer matrix.

4.4 | Short term creep tests

A typical example of axial strain response of the tested materials is shown in Figure 7 for 12.5 MPa creep stress.

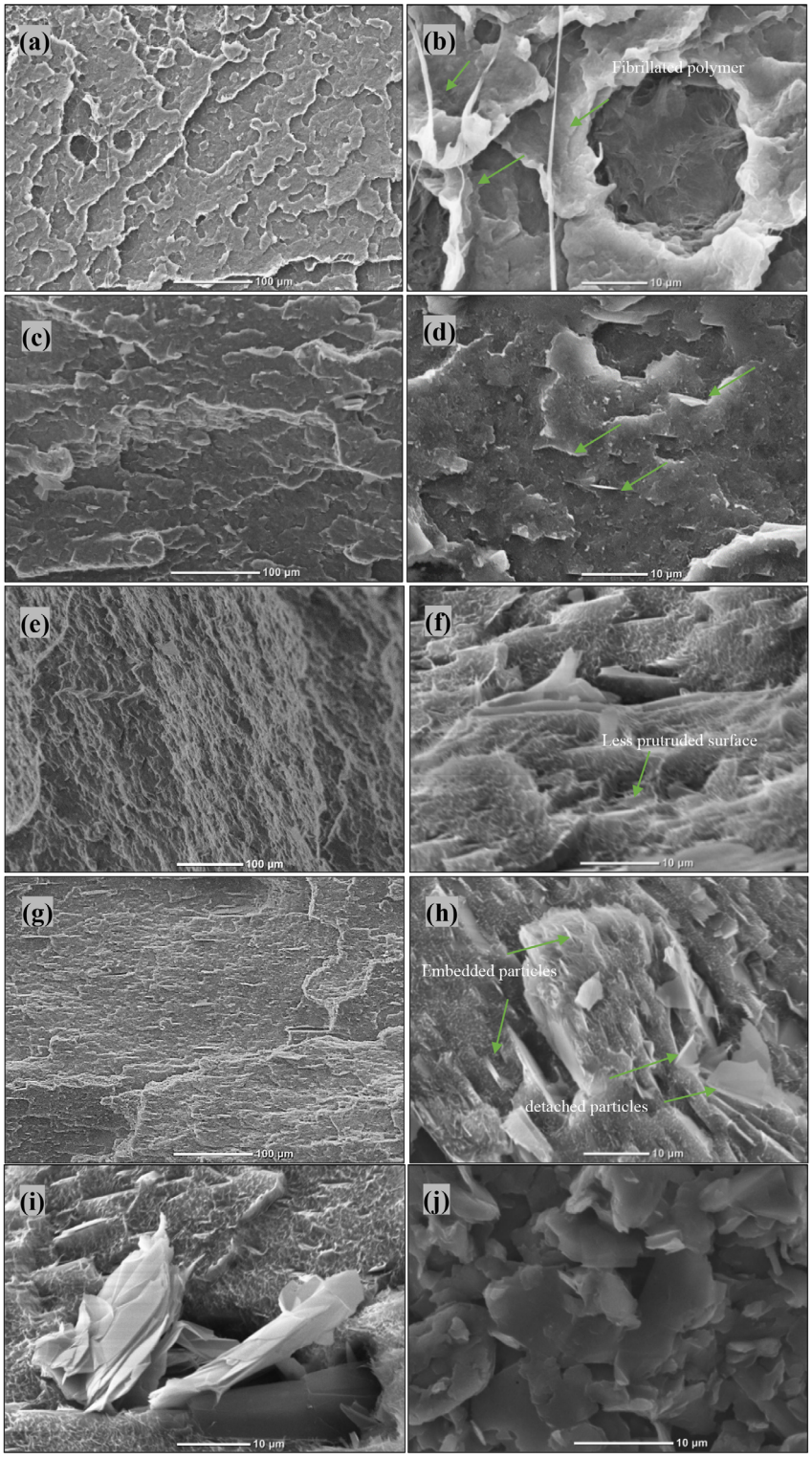

FIGURE 6 Scanning electron microscopy (SEM) micrographs of the freeze-fracture surfaces at low (left) and high (right) magnifications for (a,b) high-density polyethylene (HDPE) sample, where the arrows indicate the fibrillated surface of the neat, ductile polymer; (c,d) HDPE with 2 wt% GNPs; (e,f) HDPE with 6 wt% GNPs; and (g,h) HDPE with 15 wt% GNPs and arrows point to the platelets in the polymer; and (i,j) examples of agglomerated particles at 6% and 15% GNPs [Color figure can be viewed at wileyonlinelibrary.com]

In general, the materials show a gradual decrease in the creep and irreversible strains with the increasing amounts of the added GNPs. It can be seen that materials with high amounts GNPs recover the reversible strains faster compared to the other combinations and the pure polymer. The addition of GNPs stiffens the material and restricts the extension of the polymer chains so that they are stretched more than deformed, and thus it takes shorter times to recover after load removal. The nanoparticles participate in the increased resistance partially by replacing amount of the polymer that is prone to creep with these stiff and rigid particles that show high resistance to creep (provided a good interface between the two components exists). The interphase region

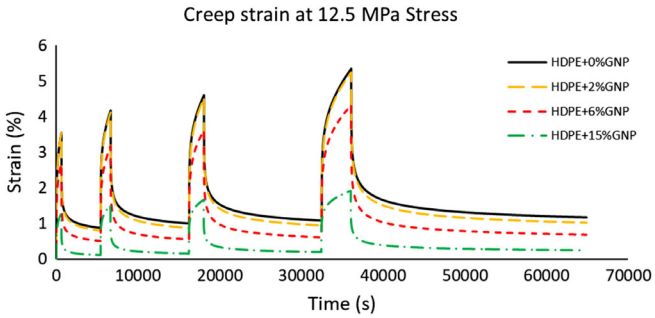

FIGURE 7 Creep strains of all samples at 12.5 MPa stress [Color figure can be viewed at wileyonlinelibrary.com]

between the polymer and the reinforcement plays a vital role in improving the resistance of the material to creep. Studies on nanoparticles such as Titania that are surface treated by organophilic modifiers compared to untreated particles for the effect on the creep behavior[41] showed that the softer organic interface resulted in minor improvements. At the same time, firmer compatibility between the reinforcement and the polymer was more effective in reducing the creep compliance of the nanocomposite. The loading-unloading-recovery test showed that 17 MPa was the critical stress level, where the stain of the HDPE+15%GNP reached around 3% (see the supporting information, Figure S2). These limits that trigger the damage were not crossed during the creep test even at the highest stress level. Also, the SEM micrographs did not show gaps at the interphase between the polymer and the particle that reduce the efficiency of the particles in improving creep resistance.

In the following, the creep response is further analyzed in terms of the VP and VE strains. Parameters are extracted for predicting the long-term behavior of the materials.

Experimental VP strains developed with time at a stress level of 10 MPa is presented in Figure 8 as symbols, showing a general trend of VP strains increasing with time and decreasing with the amount of added nanoparticles. The same trend is observed at all stress levels and can be found in Figure S3 of the supporting information. The lowest amount of VP strain was achieved at the addition of 15 wt% GNP for axial and lateral direction and for all applied stress levels. The 15 wt% GNPs is a significant amount of rigid elastic particles that are replacing quite large amount of the viscoelastic polymer resulting in a large increase of the elastic share with respect to the viscous part in the total viscoelastic response.

Modeling of the VP strains is presented as lines (solid for the axial and dotted for the lateral strain) in Figure 8. The modeling approach is capable of representing the experimental data with acceptable accuracy. Table 3 shows an evaluation of the model accuracy employing squared error value (R^2, or the coefficient of predictions) between the experimental data and the predictions of the model, where most of the data set have an R^2 higher than 0.9.

VP parameters for axial and lateral directions extracted from the experimental results for all materials are presented in Table 4. It can be seen that parameter m, which shows how VP strain develops with time in the axial direction (same for lateral), does not change significantly with the addition of GNPs. Thus, indicating that for constant stress, the dependence on time for all materials is the same in axial and lateral directions, implying that the rate of developing VP strains does not change with the addition of the nanoparticles at a constant stress level. However, the parameters which show how VP strain changes with applied stress level (i.e., M and C_{VP}) are significantly different for all materials. Correlating the individual parameter to a specific physical phenomenon is rather impossible since these are fitting parameters interlinked within the model and change together. If a general trend can be achieved, modeling materials with different content of GNPs would be possible. However, one can speculate two mechanisms underlying this behavior; one is the homogeneous distribution of the particles over the volume of the material, and the other is the good bonding between the particles and the matrix material. When particles are distributed homogeneously, the polymer chains entrapped between them behave in the same way over time and only the extent to which the VP strains changes is affected by the restricting act of the rigid particles. A similar argument applies to the change of response with the applied stress level. Assuming good bonding between the polymer and the particles, the latter share a great deal of the applied loads and further improves the resistance of the polymer to creep.

The parameters extracted from tests (Table 3) can be used to predict the VP strain development with conditions other than those used in the experiments. Results of such prediction are presented here with speculations of possible reasons for the behavior. However, these speculations are solely based on the behavior of materials in the current study and should be validated in the future. Figure 9 shows the VP strains at different stress levels (in the left figure), and at longer times than used for the test (figure to the right). For the sake of practicality, predictions were only presented for about 10 years of time under the highest loading level. After such time, the VP strains seem to be stabilizing and at the plateau, they do not exceed the critical strains determined from the loading-unloading-recovery test at which damage is expected. Curves presented earlier for the development of

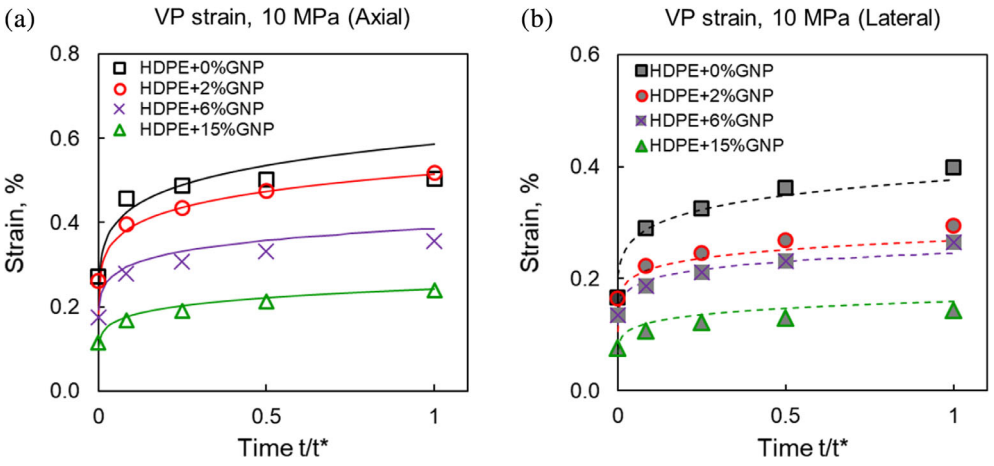

FIGURE 8 VP strain development with time for scanning electron microscopy (HDPE) with different amounts of GNPs at 10 MPa applied stress for (a) axial and (b) lateral direction due to Poisson's effect. Symbols represent experimental data points; lines represent modeling of VP strain [Color figure can be viewed at wileyonlinelibrary.com]

TABLE 3 Coefficient of predictions (squared error) between experimental data and model predictions for all tested conditions

	R^2							
	Stress (MPa)							
	7.5		10		12.5		15	
Materials	Axial	Lateral	Axial	Lateral	Axial	Lateral	Axial	Lateral
HDPE+0%GNP	0.911	0.137	0.729	0.928	0.967	0.861	0.967	0.860
HDPE+2%GNP	0.631	0.941	0.836	0.965	0.752	0.972	0.976	0.996
HDPE+6%GNP	0.989	0.937	0.973	0.920	0.982	0.879	0.506	0.705
HDPE+15%GNP	0.926	0.988	0.951	0.995	0.989	0.995	0.984	0.996

TABLE 4 VP parameters in axial and lateral directions for high-density polyethylene (HDPE) with different amounts of graphene nanoplatelets (GNP)

	Axial			Lateral		
Material	m	M	C_{VP}, %	m	m	C_{VP}, %
HDPE+0%GNP	0.13	25	$3.29 \cdot 10^{-4}$	0.11	19	$30.5 \cdot 10^{-4}$
HDPE+2%GNP	0.12	30	$1.29 \cdot 10^{-4}$	0.09	36	$1.54 \cdot 10^{-4}$
HDPE+6%GNP	0.12	23	$6.4 \cdot 10^{-4}$	0.09	28	$7.41 \cdot 10^{-4}$
HDPE+15%GNP	0.13	23	$2.47 \cdot 10^{-4}$	0.115	25	$2.13 \cdot 10^{-4}$

the VP strains from loading-unloading-recovery test are also presented here for comparison. Both tests showed the same trend of reduced damage at higher content of reinforcement. However, it can be seen that for the same stress level, extended loading time (creep) results in much larger VP strains than the shorter loading does. On the other hand, the slope of the curves tends to change dramatically with a steeper increase in the loading-unloading-recovery test after a certain stress level (around 20 MPa), indicating that damage might start later, but it results in more significant changes than in case of creep test (where the effect of microdamage is neglected during modeling). A possible scenario is that with the creep test, there is still time for the polymer molecules to rearrange and elongate further, but this is not possible at higher rates, leading to failure of interphase. This, however, is speculation that cannot be confirmed here based on the available data. Moreover, it is reported that extrapolating creep curves to stresses higher than those used in the test is sensitive to changes in the VP parameters and thus should further be investigated.[42]

After viscoplasticity has been analyzed, it is possible to subtract it from the total strain in order to obtain pure VE strain. The curves for VE strain development and creep compliance for all the different loading times for HDPE +2% GNP at 15 MPa applied stress level are presented in Figure 10. It can be seen that for all the loading time durations, the VE strain and creep compliances follow the same curve and increase in value with time. This trend was observed for all stress levels, indicating good repeatability of

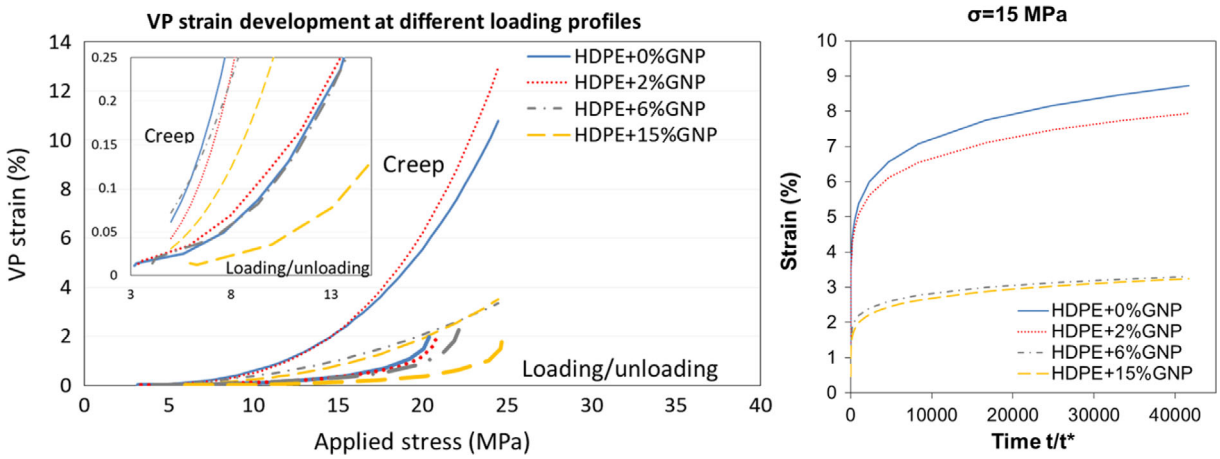

FIGURE 9 Development of VP strain with respect to stress at different loading profiles (left). Thin trendlines represent the VP strains from creep test and thick ones belong to the loading-unloading-recovery test, and prediction of VP strains for times longer than those used in the test (right). T/t* = 40,000 is slightly below 10 years [Color figure can be viewed at wileyonlinelibrary.com]

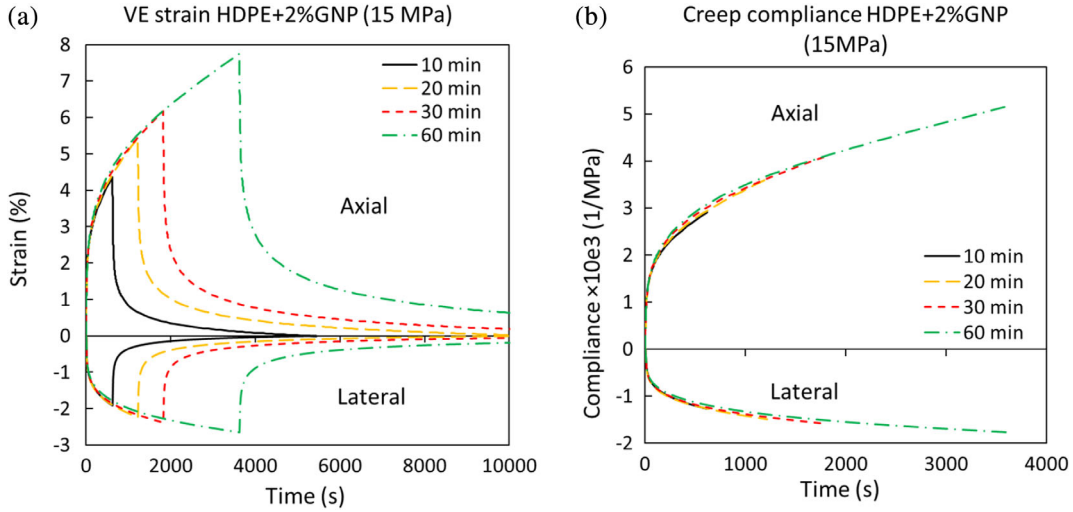

FIGURE 10 Development of pure VE strain (a) and creep compliance (b) with time for HDPE +2 wt% GNP for different loading durations at 15 MPa applied stress level in the axial direction and the lateral response as a result of Poisson's effect [Color figure can be viewed at wileyonlinelibrary.com]

the experiment with different applied times. It should be noted that smaller offsets of this trend could be observed at higher stress levels and lateral strain (Figure 10). Samples of HDPE and its nanocomposites have very smooth surfaces, and it is challenging to adhere to other surfaces, which makes it problematic to assure proper contact of strain gages for accurate lateral strain reading at higher stress levels. Employing a digital image correlation for lateral strain measurements would be a solution to overcome this problem. Overall, the same trend could be observed with all the materials and all stress levels, but only data for stress level of 15 MPa are presented here for the sake of the space. Graphs from other applied creep stresses could be found in the supporting information in Figures S4 through S7.

Comparison between different stress levels of pure VE strain and creep compliances for HDPE+15 wt% GNP are shown in Figure 11. It can be observed that with the increase of applied creep stress, the VE strain curves are steeper and with much higher values. The data of creep compliances indicate that even at very low stress of 10 MPa, the material is nonlinearly viscoelastic (a general trend for all studied materials), thus modeling of viscoelasticity for such materials must be performed with nonlinear VE models, for example, Schapery type of model.[43–45] Modeling the viscoelasticity would allow extracting additional parameters describing the VE response of materials with time and stress. Combined with the VP parameters, total behavior of a material can then be predicted at any complex loading profile.

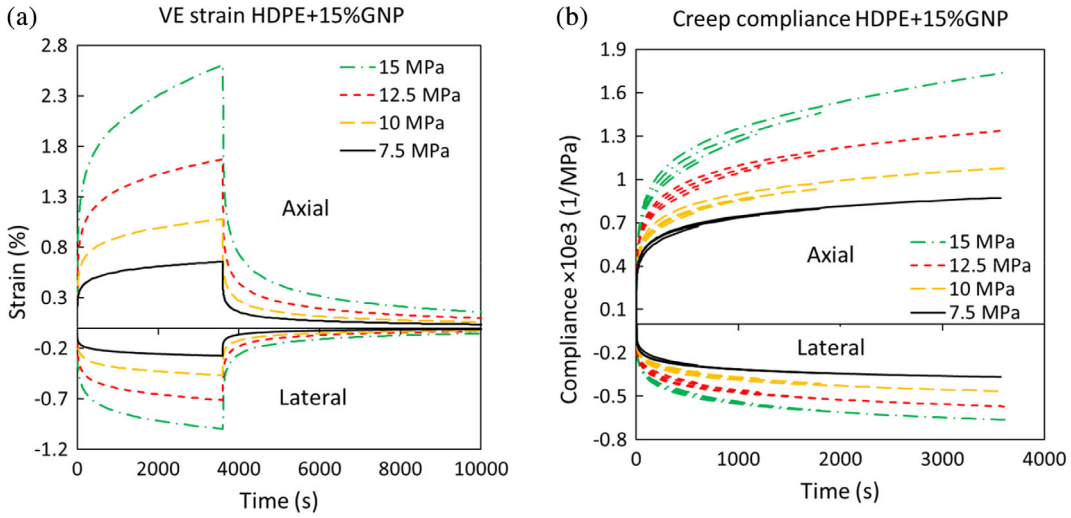

FIGURE 11 Development of pure VE strain (a) and creep compliance (b) for HDPE +15 wt% GNP at different applied stresses at 60 min loading duration in the axial direction and the response in the lateral direction as a result of Poisson's effect [Color figure can be viewed at wileyonlinelibrary.com]

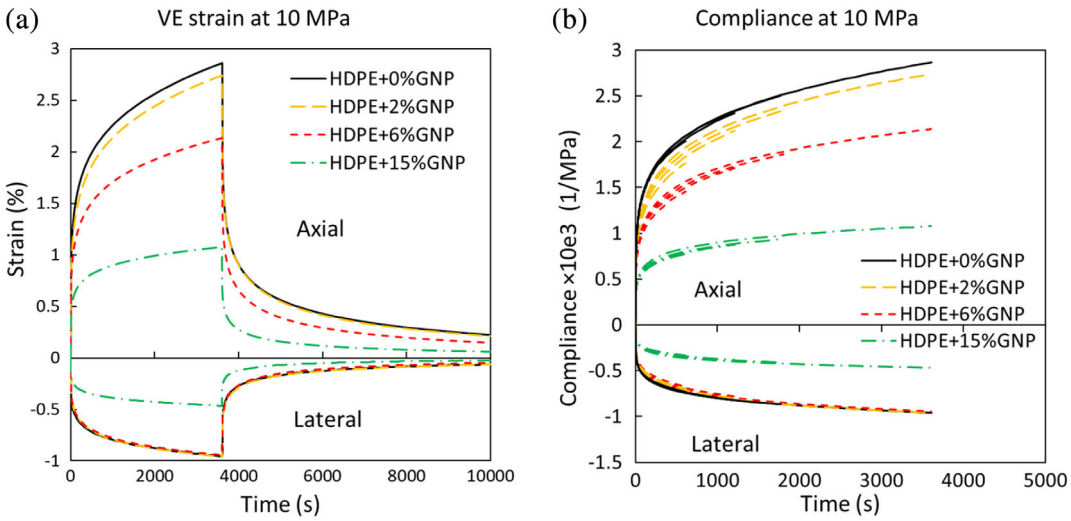

FIGURE 12 Pure VE strain (a) and creep compliances (b) for HDPE with different GNP content at 10 MPa applied stress in the axial direction and lateral response due to Poisson's effect [Color figure can be viewed at wileyonlinelibrary.com]

Comparison of different materials shows a similar trend to viscoplasticity, as shown in Figure 12, where pure VE strain and creep compliances at 10 MPa are shown. HDPE with 15 wt% GNP shows more than 60% lower amounts of VE strain than pure HDPE in the axial and the lateral direction. Follows is HDPE+6%GNP and HDPE with 2 wt% GNP with axial strain reduction of ∼27% and 2.5%, respectively. This trend is directly related to the amount of the added nanoplatelets by the stiffening effect and the reduced amount of polymer chains to be stretched. For particular applied stress, the sample with the maximum amount of GNPs reaches the stable strain faster and likewise recovers it. The other combinations show a tendency to further stretch at the end of the loading time.

5 | CONCLUSIONS

Time-dependent properties were investigated on nanocomposites manufactured from commercial materials in the form of masterbatch and using an industrial-relevant process. The selected form of material and processing method resulted in scalable composites with good distribution and dispersion of the nanoparticles without handling hazardous dry nanoparticles.

Two tests with different loading profiles were performed on HDPE doped with various GNP amounts to characterize their viscoplastic properties and evaluate the effect of nano-reinforcement on viscoplasticity parameters, where results showed an explicit dependency on the loading history and the recovery time. The addition of GNPs resulted in a significant improvement in the creep resistance of the polymer by restricting the mobility and deformation of the molecular chains, especially at high GNP loadings (at 15 wt% GNP), where the creep strains were reduced by more than 50% at all stress levels in the axial direction and about 40% in their lateral response. Results from both tests were consistent and supported by morphological observations.

The behavior of materials was reproduced with high accuracy using the Zapas model. This model was later applied to predict the VP strain development at times significantly longer than that used in the test. The viscoelastic/viscoplastic strain components were separated and analyzed. It was evident that the nanocomposites exhibit a nonlinear elastic and viscoelastic response even at low applied stresses. According to that, suitable approaches have been proposed to model their response. Analysis of stiffness evolution with applied stress indicated that stress of 17 MPa is a critical value. After this stress level, the accumulated damage and filler-filler interactions result in the degradation of the mechanical response.

The used approach of gathering modeling parameters of viscoplastic and viscoelastic response, together with evaluating critical stress level, provide valuable information for material selection during design of polymer parts for applications where time-dependent properties are essential.

ACKNOWLEDGMENTS

Part of this study was financially supported by Interreg Nord project "Smart WPC" (funded by EU and Region Norrbotten) and project Smart Machine and Materials (SMM) within the excellence and innovation area at Luleå University of Technology. The project Nano2Day (grant agreement no. 777810) is also acknowledged. Authors would like to thank Runar Långström and Robert Westerlund at RISE SICOMP for composites processing and the help from Diego Carrasco Fernández (project student at LTU) in performing the creep experiment.

ORCID

Zainab Al-Maqdasi https://orcid.org/0000-0001-5550-2962
Liva Pupure https://orcid.org/0000-0001-8050-2294
Guan Gong https://orcid.org/0000-0003-3449-8233
Nazanin Emami https://orcid.org/0000-0001-8676-8819
Roberts Joffe https://orcid.org/0000-0002-5210-4341

REFERENCES

[1] K. Friedrich, A. A. Almajid, *Appl. Compos. Mater.* **2013**, *20*, 107.
[2] K. Friedrich, *Adv. Ind. Eng. Polym. Res.* **2018**, *1*, 3.
[3] V. Mara, R. Haghani, P. Harryson, *Constr. Build. Mater.* **2014**, *50*, 190.
[4] A. Mirabedini, A. Ang, M. Nikzad, B. Fox, K. T. Lau, N. Hameed, *Adv. Sci* **2020**, *7*, 1903501.
[5] B. Arash, W. Exner, R. Rolfes, *J. Mech. Phys. Solids* **2019**, *128*, 162.
[6] O. Starkova, J. Yang, Z. Zhang, *Compos. Sci. Technol.* **2007**, *67*, 2691.
[7] Z. Zhang, J. L. Yang, K. Friedrich, *Polymer (Guildf).* **2004**, *45*, 3481.
[8] V. Devasenapathi, P. Monish, S. P. Balasivanandha, *Int. J. Adv. Manuf. Technol.* **2009**, *44*, 412.
[9] R. D. Maksimov, J. Bitenieks, E. Plume, J. Zicans, R. M. Merijs, *Mech. Compos. Mater.* **2010**, *46*, 237.
[10] J. Zicans, R. M. Merijs, M. Kalniņš, R. Maksimovs, J. Jansons, ZAMM Zeitschrift fur Angew, *Math. Und Mech.* **2015**, *95*, 1198.
[11] L.-C. Tang, X. Wang, L.-X. Gong, K. Peng, L. Zhao, Q. Chen, L.-B. Wu, J.-X. Jiang, G.-Q. Lai, *Compos. Sci. Technol.* **2014**, *91*, 63.
[12] A. Zandiatashbar, C. R. Picu, N. Koratkar, *Small* **2012**, *8*, 1676.
[13] C. Lee, X. Wei, J. W. Kysar, J. Hone, *Science* **2008**, *321*, 385.
[14] Y. Zhu, S. Murali, W. Cai, X. Li, J. W. Suk, J. R. Potts, R. S. Ruoff, *Adv. Mater.* **2010**, *22*, 3906.
[15] A. A. Balandin, S. Ghosh, W. Bao, I. Calizo, D. Teweldebrhan, F. Miao, C. N. Lau, *Nano Lett.* **2008**, *8*, 902.
[16] J. T. Hope, W. Sun, S. Kewalramani, S. Saha, P. Lakhe, S. A. Shah, M. J. Mason, M. J. Green, R. A. Hule, *ACS Appl. Nano Mater.* **2020**, *3*, 10303.
[17] T. Gkourmpis, K. Gaska, D. Tranchida, A. Gitsas, C. Müller, A. Matic, R. Kádár, *Nanomaterials* **2019**, *9*, 1766.
[18] X. Zhao, Q. Zhang, D. Chen, P. Lu, *Macromolecules* **2010**, *43*, 2357.
[19] D. G. Papageorgiou, I. A. Kinloch, R. J. Young, *Prog. Mater. Sci.* **2017**, *90*, 75.
[20] O. Starkova, S. T. Buschhorn, E. Mannov, K. Schulte, A. Aniskevich, *Compos. Part A Appl. Sci. Manuf.* **2012**, *43*, 1212.
[21] T. Glaskova-Kuzmina, A. Aniskevich, M. Zarrelli, A. Martone, M. Giordano, *Compos. Sci. Technol.* **2014**, *100*, 198.
[22] F. H. Norton, *The creep of steel at high temperatures*, Forgotten Books, London **1929**.
[23] A. Muliana, *Int. J. Solids Struct.* **2014**, *51*, 122.
[24] L. J. Zapas, J. M. Crissman, *Polymer (Guildf).* **1984**, *25*, 57.
[25] L. O. Nordin, J. Varna, *Compos. Part A Appl. Sci. Manuf.* **2006**, *37*, 344.
[26] E. Marklund, J. Varna, L. Wallström, J. Eng, *Mater. Technol.* **2006**, *128*, 527.
[27] L. Rozite, J. Varna, R. Joffe, A. Pupurs, J. Thermoplast, *Compos. Mater.* **2013**, *26*, 476.
[28] L. Pupure, J. Varna, R. Joffe, *Adv. Compos. Lett* **2015**, *24*, 125.
[29] K. Giannadakis, J. Varna, *Compos. Part A Appl. Sci. Manuf.* **2014**, *62*, 67.

[30] Group NanoXplore, heXo-G V Product Datasheet, https://www.nanoxplore.ca/wp-content/uploads/2017/11/Datasheet_hexo-G_V_20161027-nanoxplore-products.pdf, **2021**.
[31] Z. Al-Maqdasi, G. Gong, B. Nyström, N. Emami, R. Joffe, *Materials (Basel)* **2020**, *13*, 2089.
[32] K. Kalaitzidou, H. Fukushima, L. T. Drzal, *Compos. Sci. Technol.* **2007**, *67*, 2045.
[33] N. Dusunceli, B. Aydemir, *J. Elastomers Plast.* **2011**, *43*, 451.
[34] J. Kolařík, A. Pegoretti, *Polymer (Guildf).* **2006**, *47*, 346.
[35] K. Alasvand Zarasvand, H. Golestanian, *Compos. Sci. Technol.* **2017**, *139*, 117.
[36] C. L. Beatty, F. E. Karasz, J. Macromol, *Sci. Rev. Macromol. Chem.* **1979**, *17*, 37.
[37] C. Hershey, K. Jayaraman, J. Polym, *Sci. Part B Polym. Phys.* **2019**, *57*, 62.
[38] W. J. Boo, J. Liu, H. J. Sue, *Mater. Sci. Technol.* **2006**, *22*, 829.
[39] B. Vergnes, *Int. Polym. Process* **2019**, *34*, 482.
[40] R. Adhikari, G. H. Michler, *Polym. Rev.* **2009**, *49*, 141.
[41] F. Bondioli, A. Dorigato, P. Fabbri, M. Messori, A. Pegoretti, *J. Appl. Polym. Sci.* **2009**, *112*, 1045.
[42] L. Pupure, J. Varna, R. Joffe, *J. Compos. Mater.* **2016**, *50*, 575.
[43] Y. C. Lou, R. A. Schapery, J. Compos, *Mater.* **1971**, *5*, 208.
[44] R. Schapery, *Further development of a thermodynamic constitutive theory: stress formulation*, Purdue Research Foundation, Lafayette **1969**.
[45] R. A. Schapery, *Polym. Eng. Sci.* **1969**, *9*, 295.

SUPPORTING INFORMATION

Additional supporting information may be found online in the Supporting Information section at the end of this article.

How to cite this article: Al-Maqdasi Z, Pupure L, Gong G, Emami N, Joffe R. Time-dependent properties of graphene nanoplatelets reinforced high-density polyethylene. *J Appl Polym Sci*. 2021; e50783. https://doi.org/10.1002/app.50783